

Microwave micro-plasmas in air: simulations and experiment

P. Coche¹, V. Guerra¹, K. Gadonna², G.D. Stancu³, O. Leroy², T. Minea² and L.L. Alves¹

¹*Instituto de Plasmas e Fusão Nuclear, Instituto Superior Técnico,
Universidade de Lisboa, Portugal*

²*LPGP, UMR 8578: CNRS-Université Paris-Sud, 91405 Orsay, France*

³*CentraleSupélec, EM2C, CNRS UPR 288, Grande Voie des Vignes, 92295
Châtenay-Malabry, France*

1. Introduction

Micro-plasmas generated in capillaries have recently aroused research interest in several fields like photonics, medicine and plasma-surface processing. Here, we report on very recent experimental and modelling results, obtained from the study of micro-plasmas generated in dry air (N₂ 80% - O₂ 20%) using microwaves (2.45 GHz excitation frequency and ~100 W coupled power), confined within a small radius capillary ($R=345\text{ }\mu\text{m}$) at low pressure ($p=300\text{ Pa}$).

2. Modelling

The simulations are performed using the in-house IST-LoKI (LisbOn KInetics) numerical code, which keeps the same algorithmic structure and calculation blocks used in previous publications [1,2]. The 0D (volume averaged) model couples the homogeneous two-term electron Boltzmann equation (EBE) (for the gas mixture considered, including first and second kind collisions) to a system of rate balance equations for molecules N₂(X, v=0-59), N₂(A, B, C, a, a', w), O₂(X, a, b), NO(X, A, B), NO₂(X, A), O₃, O₃*; atoms N(⁴S, ²D, ²P) and O(³P, ¹D); positive ions N⁺, N₂⁺(X, B), N₃⁺, N₄⁺, O⁺, O₂⁺ and NO⁺; and negative ion O⁻. All cross sections used are or will be available in the near future, at the IST-LISBON database of LXCat [3].

Working at low pressure (< 1000 Pa) and low radius (< 500 μm) results in a high reduced electric field and a non-classical ambipolar transport for charged particles. To meet these conditions, the kinetic-energy working-grid in the EBE was extended up to 1000 eV, to describe the effect of the high-energy mechanisms impacting significantly on the tail of the electron energy distribution function, and a transport theory was developed for pR values beyond the validity limit of the classical ambipolar theory. Under our typical operating conditions (electron density $n_e \approx 4 \times 10^{12}\text{ cm}^{-3}$, gas temperature $T_g \approx 1000\text{ K}$ and electron temperature $T_e \approx 4-7\text{ eV}$), we have $\Lambda/\lambda_D \approx 15$ ($\Lambda = R/2.405$ is the diffusion length for infinite cylindrical geometry and λ_D is the Debye length) corresponding to a dense plasma in

“ambipolar regime”, and $\Lambda/\lambda_i \sim 0.5$ (λ_i is the ion mean-free-path) corresponding to low-pressure. A transport theory embedding the transition from low to high pressures in dense plasmas was derived by Self and Ewald [4] and later revisited by Ferreira and Ricard [5], for a single type of positive ion. Here, we have generalized the theory of Self and Ewald for N₂-O₂ mixtures at low pressure, accounting for several positive ions and one (low-density) negative ion species (listed at the beginning of this section), recovering a system of equations formally identical to the one of [4], whose numerical solution can be avoided using the results of [5] as an abacus.

Figure 1 shows the self-consistent calculated values of the reduced electric field, E/N , and of the electron kinetic temperature, T_e , as a function of R , using three different descriptions for the charged-particle transport: the current formulation for several positive ions and one negative ion; the current formulation neglecting the effect of negative ions; and the classical ambipolar diffusion.

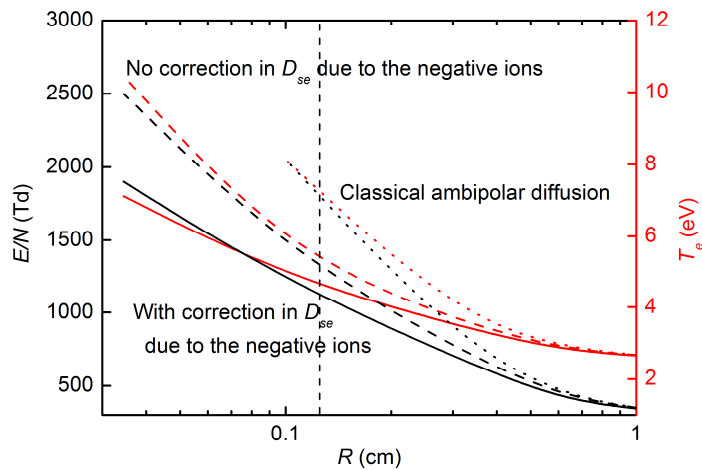


Figure 1: Reduced electric field (left axis, black) and electron temperature (right axis, red) for $p=300$ Pa, $T_g=1100$ K and $n_e=3.84 \times 10^{12}$ cm⁻³, as a function of the tube radius, calculated using: the present theory (full line); the present theory neglecting the effect of negative ions (dashed line); the classical ambipolar theory (dotted line). The short-dashed vertical line limits the R -region of low-pressure conditions.

Our model calculations in the presence of O⁻ ions should be restricted to low-pressures ($\Lambda/\lambda_i \leq 1$, corresponding to $R \leq 0.12$ cm), i.e., to the region on the left of the short-dashed vertical line. However, as R increases the influence of negative ions becomes negligible and the present formulation can still be used, albeit with caution. Moreover, the different transport descriptions considered yield similar results at high R , thus confirming the classical ambipolar diffusion limit at $\Lambda/\lambda_i \gg 1$.

3. Experiment

The experimental setup, operating at LPGP, is represented in figure 2 (more details in [6]).

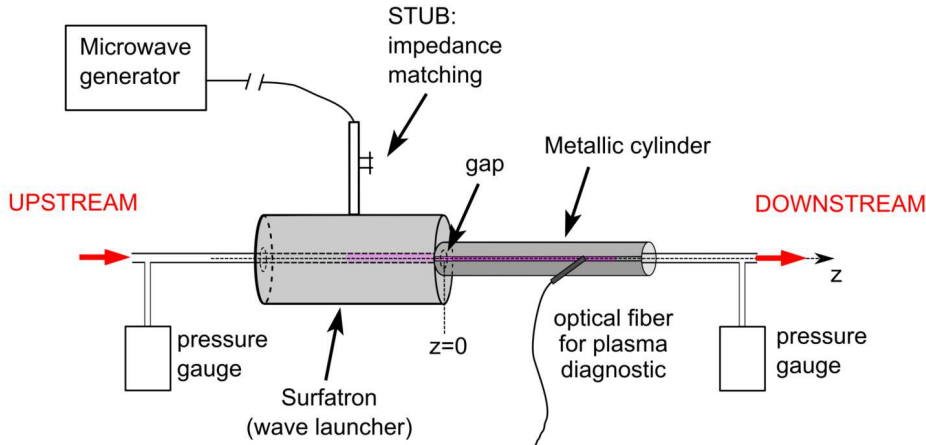


Figure 2: Schematic representation of the experimental setup.

The capillary is inserted into a surfatron especially adapted to the system geometrical dimensions, ensuring a maximum electric field at the gap. Dry air is introduced from the left end of the capillary, at negligible gas flow, yielding a constant pressure along the plasma column. Non-intrusive axially-resolved optical emission spectroscopy (OES) diagnostics are used to obtain: (i) the electron density, measured from the contribution of the Stark effect to the broadening of the Balmer line H_{β} (486.1 nm), which provides an upper-limit estimation $n_e < 1.4 \times 10^{13} \text{ cm}^{-3}$. The latter agrees with a semi-empirical analysis of the power coupled to the plasma, based on the solution to Maxwell's equations for the excitation structure; (ii) the absolute densities of $\text{N}_2(\text{C})$, $\text{N}_2(\text{B})$, $\text{N}_2^+(\text{B})$, $\text{N}(3\text{p}^4\text{S})$ and $\text{O}(3\text{p}^5\text{P})$, and the relative intensities of the second positive system $\text{N}_2(\text{C},v) \rightarrow \text{N}_2(\text{B},v')$ (whose spectrum is used to determine also the rotational/gas temperature), the first negative system $\text{N}_2^+(\text{B},v) \rightarrow \text{N}_2^+(\text{X},v')$, and the atomic transitions $\text{N}(3\text{p}^4\text{S}) \rightarrow \text{N}(3\text{s}^4\text{P})$ and $\text{O}(3\text{p}^5\text{P}) \rightarrow \text{O}(3\text{s}^5\text{S})$. The absolute calibration of the spectra was performed at EM2C, using a standard tungsten lamp for which the spectral radiance is known. The same detection system (including the spectrometer and the optical collection system) is employed for recording both the discharge and the lamp spectra, the former being converted in radiance units by using the sensitivity response function. The gas temperature and the absolute density of a particular electronic excited state are obtained by comparing measured and Specair-simulated [7] spectra.

4. Results and discussion

Figure 2 compares measurements and simulations of (i) the relative intensity with the atomic transition of triplets $\text{N}(3\text{p}^4\text{S}) \rightarrow \text{N}(3\text{s}^4\text{P})$ and $\text{O}(3\text{p}^5\text{P}) \rightarrow \text{O}(3\text{s}^5\text{S})$ and (ii) the absolute densities

of $N_2(C)$, $N_2(B)$ and $N_2^+(B)$, as a function of the axial position in the plasma column. Model results are in qualitative agreement with measurements, predicting the correct trend for the axial evolution of the atomic line transitions and under- / over- estimating the densities of $N_2(B,C) / N_2^+(B)$ by factors below 10 times.

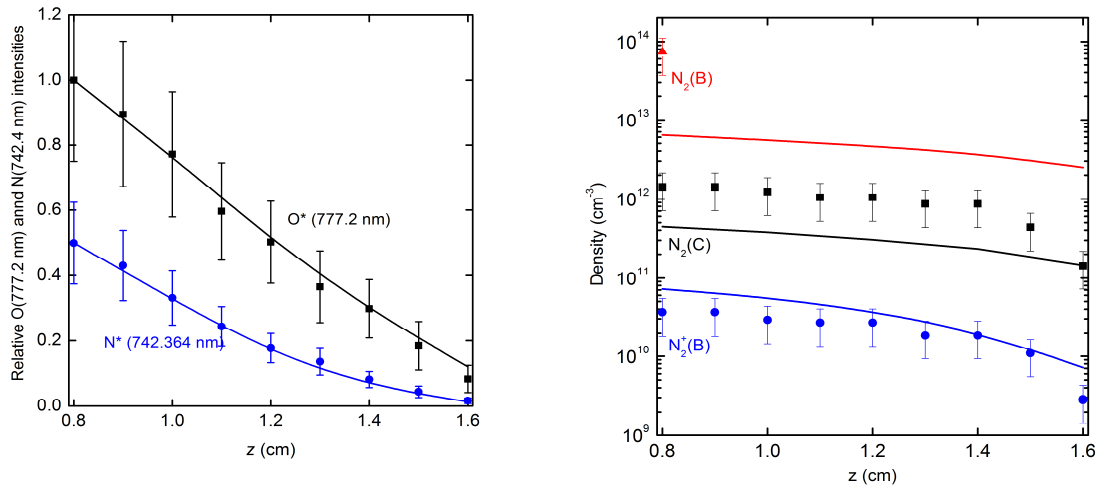


Figure 2. Axial profiles, calculated (lines) and measured (points) at 129 W coupled power, for: left, the relative intensities with atomic line transitions $N(3p^4S) \rightarrow N(3s^4P)$ (blue) and $O(3p^5P) \rightarrow O(3s^5S)$ (black); right, the absolute densities of $N_2(C)$ (black), $N_2(B)$ (red) and $N_2^+(B)$ (blue).

5. Final remarks

A low pressure, small radius microwave micro-plasma discharge has been analysed, using both simulations and measurements. Under these work conditions, the charge-particle transport description, including the effect of one negative ion species, has been successfully developed. OES diagnostics were employed to measure the absolute densities of several species and the relative intensities of some radiative transitions. Simulation results evidence good qualitative agreement with measurements.

6. Acknowledgements

This work was partially supported by FCT - Fundação para a Ciência e a Tecnologia, under Project UID/FIS/50010/2013 and Project PLASMA-ADIST, and by the Labex LaSIPS, under Project MicroCap.

7. References

- [1] V. Guerra and J. Loureiro, *Plasma Sources Sci. Technol.* **6** (1997) 373
- [2] V. Guerra and J. Loureiro, *Plasma Sources Sci. Technol.* **8** (1999) 110
- [3] L.L. Alves, *J. Phys.: Conf. Ser.* **565** (2014) 012007; www.lxcat.net
- [4] S.A. Self and H.N. Ewald, *Phys. Fluids* **9** (1966) 2486
- [5] C.M. Ferreira and A. Ricard, *J. Appl. Phys.* **54** (1983) 2261
- [6] S. Dap et al, *Plasma Sources Sci. Technol.* (2015) submitted
- [7] Specair www.specair-radiation.net